12.2 ON THE MOTION AND INTERACTION BETWEEN LEFT- AND RIGHT-MOVING SUPERCELLS ON 4 MAY 2003

Daniel T. Lindsey[1*] and Matthew J. Bunkers[2]
[1]Cooperative Institute for Research in the Atmosphere
Fort Collins, Colorado
[2]NOAA/National Weather Service Forecast Office
Rapid City, South Dakota

1. INTRODUCTION

Mergers between left- and right-moving supercells have received relatively little attention in the literature. Several studies have discussed, or briefly mentioned, the effects of mergers on tornadogenesis (Stout and Hiser 1955; Bluestein and Parker 1993; Finley et al. 2001; Dowell and Bluestein 2002), but few have focused specifically on left-mover/right-mover mergers. On 4 May 2003, a left-moving supercell interacted with a right-moving supercell in extreme northeastern Oklahoma and southwestern Missouri. A tornado was reported with the right mover prior to the merger, and again after the left mover exited the area, but there were no tornado reports during and immediately following the merger.

This paper will begin by discussing the synoptic setup for the severe weather outbreak on 4 May 2003, then examine the mesoscale environment in which the storms of interest formed and moved through. The next section will discuss the anomalous motions of the supercells, and the final section will detail their merger and introduce some possible reasons why the right mover's tornadic circulation was disrupted.

2. SYNOPTIC ENVIRONMENT

At 1200 UTC 4 May 2003, a 300 hPa longwave trough axis was located near the Arizona/New Mexico border, while a 130 knot jet streak at 300 hPa had rounded the trough and was progressing northeastward (Fig. 1a, b). By 0000 UTC on 5 May, the trough had become negatively tilted and its axis had moved eastward to Kansas and Oklahoma. At the surface, a 995 hPa low pressure center was located over western Kansas at 12:00 UTC; by 0000 UTC it had moved eastward to near the Kansas/Missouri border. A dryline—characterized by a 17 °C (30 °F) dewpoint temperature difference—(Fig. 1 c, d; Fig. 3) moved from western Oklahoma at 1200 UTC to central Oklahoma by 0000 UTC. Dew point values in the warm sector in eastern Oklahoma and southwestern Missouri were in the lower 20's °C (lower 70's °F).

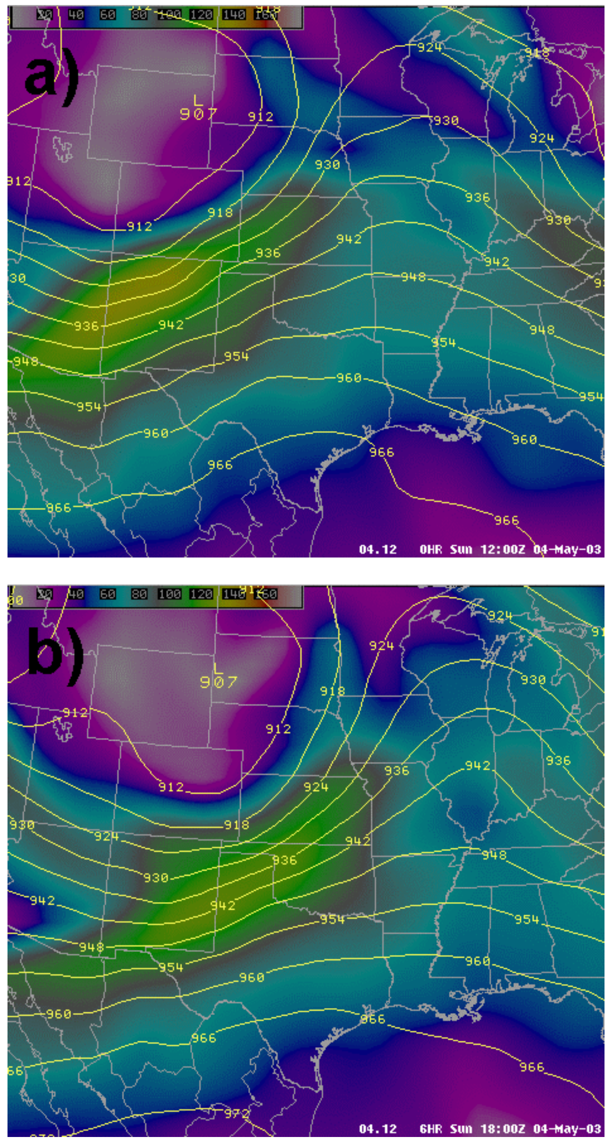

Corresponding author address: Daniel T. Lindsey, CIRA/Colorado State University, 1375 Campus Delivery, Ft. Collins, CO 80523-1375; email: lindsey@cira.colostate.edu

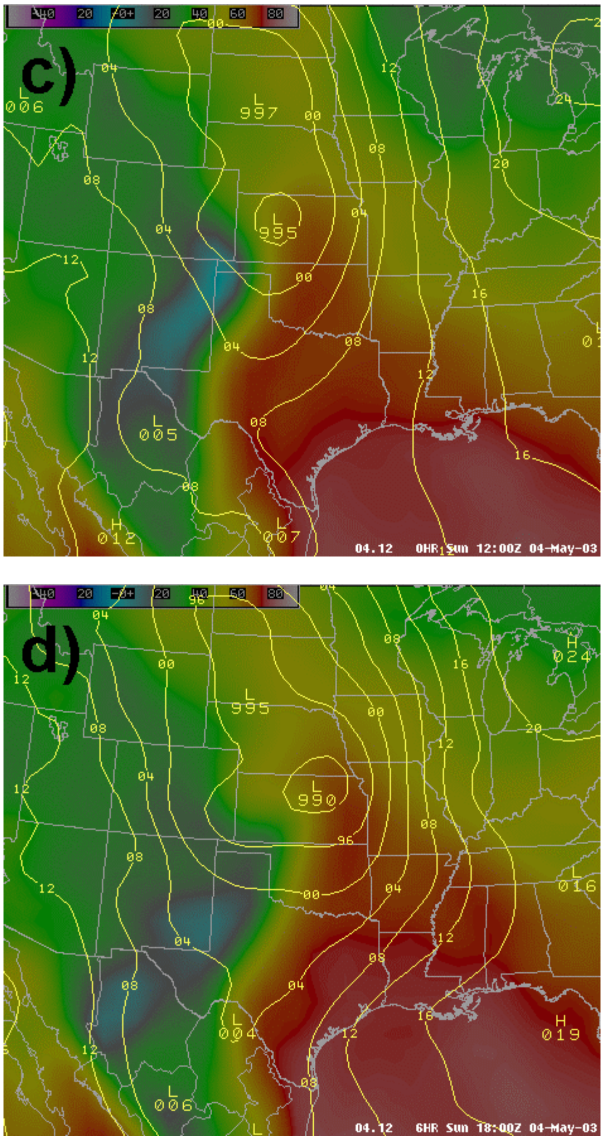

Figure 1. a, b) ETA 300 hPa heights (yellow contours) and wind speed (colors). c, d) ETA surface SLP (yellow contours) and dew point (colors) at 12:00 UTC 4 May 2003 for a, c), and 00:00 UTC 5 May 2003 for b, d).

A special sounding at Norman, OK (1800 UTC 4 May 2003, Fig. 2) and the routine sounding at Springfield, MO (0000 UTC 5 May 2003) indicated the MLCAPE was 2346 J kg^{-1} and 2143 J kg^{-1}, respectively (MLCAPE is herein defined as the CAPE computed by mixing the lowest 1000 m of the environment, then lifting a parcel from this layer). Midlevel dry air capped a warm and moist boundary layer near 800 hPa (Fig. 2); however, convective inhibition was still less than 15-25 J kg^{-1}. This instability, combined with 0–6-km AGL bulk shear of 35 m s^{-1} (70 kt), suggested the environment was highly conducive to supercells (e.g., Rasmussen and Blanchard 1998). Indeed, thunderstorms developed rapidly along a surface convergence line in northeastern Kansas by 1900 UTC (Fig. 3), many of which eventually developed supercellular characteristics.

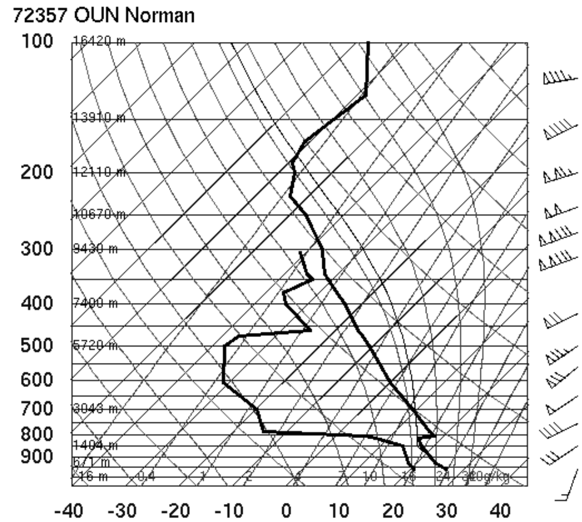

Figure 2. Sounding from Norman, Oklahoma at 1800 UTC 4 May 2003 (courtesy of the University of Wyoming).

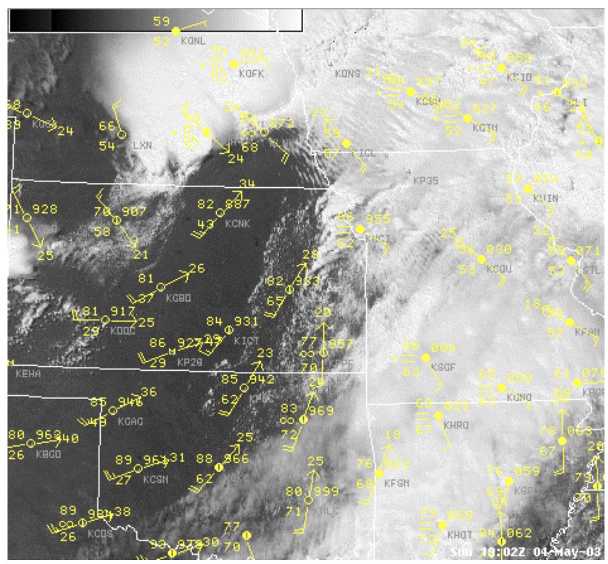

Figure 3. GOES-12 visible satellite image (1902 UTC 4 May 2003) overlaid with surface observations (1900 UTC 4 May 2003).

3. SUPERCELL EVOLUTION

An area of thunderstorms initiated in southeastern Oklahoma on the southern end of a convergence line shortly after 2000 UTC, with storm splitting occurring between 2041 and 2111 UTC per the Weather Surveillance Radar-1988 Doppler (WSR-88D) at Tulsa, Oklahoma; GOES-12 satellite images were also able to depict the split between 2045 and 2145 UTC (Fig. 4).

The right-moving[1] supercell in southeastern Oklahoma progressed east-northeastward and took on a classic supercellular appearance (as viewed from the KINX radar, not shown), while the left mover tracked rapidly northeastward. A second group of thunderstorms formed along the dryline in northeastern Oklahoma around 2030 UTC, and another right-moving supercell progressed east-northeastward toward the northeastern corner of Oklahoma (Fig. 4a-f). By 2302 UTC, the rapidly moving left-moving supercell was about to collide with the tornadic right-mover in extreme northeastern Oklahoma; this interaction will be discussed in section 4. Using radar data from KINX, the left-moving supercell's motion was 219° at 34 m s^{-1} (66 kt) from 2100-2300 UTC, while the motion of right-moving supercell in extreme northeastern Oklahoma was 256° at 21 m s^{-1} (40 kt).

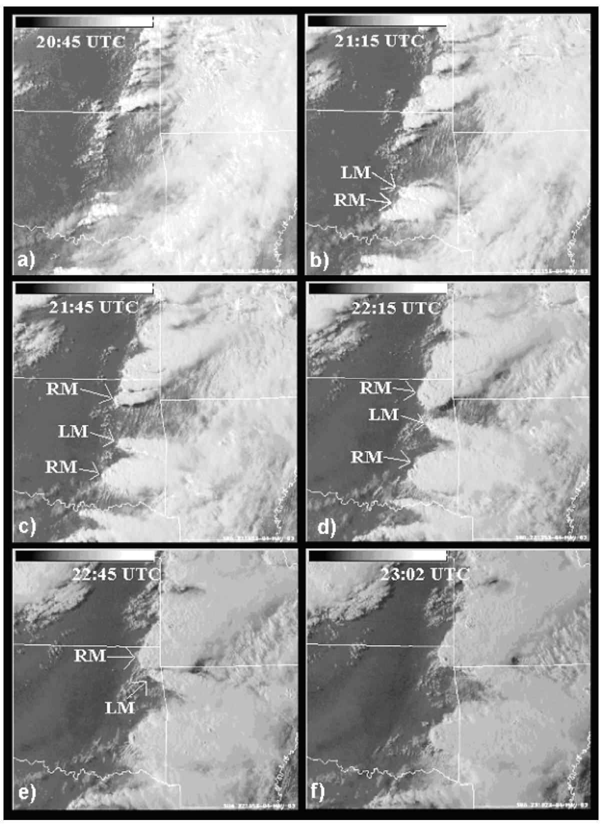

Figure 4. GOES-12 visible satellite progression at a) 2045 UTC, b) 2115 UTC, c) 2145 UTC, d) 2215 UTC, e) 2245 UTC, and f) 2302 UTC 4 May 2003. 'LM' and 'RM' point toward the left-moving and right-moving storms discussed in the text.

The wind profiler near Haskell, Oklahoma (HKL; see Fig. 7a for location) is situated in an ideal location for obtaining the wind field into which the supercells moved, particularly the left mover. Fig. 5 is the hodograph from HKL at 2100 UTC, about 1 hour before the left mover passed within a few miles of the profiler. To a first-order approximation the hodograph is a straight line from the surface to 3 km, which engenders splitting supercells. Positive values of storm-relative helicity (SRH) for the right mover and negative values of SRH for the left mover are favorable for the maintenance of both storm types (Davies-Jones et al. 2001). However, there are some important, yet subtle, hodograph curvature characteristics in the lowest levels. First, the surface–2-km hodograph curves in a clockwise direction, while the hodograph in the 2–4-km layer exhibits counter-clockwise curvature. This low-level clockwise curvature is favorable for tornadogenesis in the right mover, but unfavorable for the left mover since positive streamwise vorticity would enter the left-mover's updraft near the surface (Davies-Jones et al. 2001). Accordingly, the 0–1-km SRH was 157 $m^2 s^{-2}$ (-46 $m^2 s^{-2}$) given the observed motion of the tornadic right-moving (nontornadic left-moving) supercell. Thompson et al. (2003) found that similar values of positive 0–1-km SRH are favorable for supercells producing significant tornadoes. Lastly, the counter-clockwise curvature from 2–4-km apparently was not a detrimental factor to the sustenance of right-moving supercells. However, this "reverse S-shaped" hodograph configuration still demands further investigation because it has not been adequately addressed in modeling studies, and it may be important from a forecasting perspective.

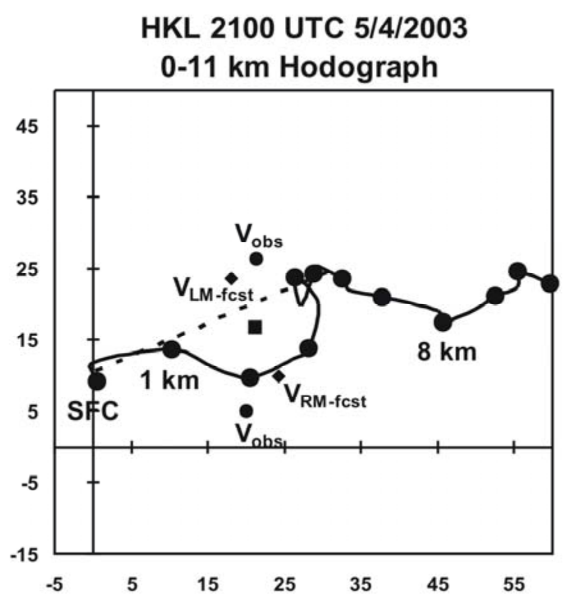

Figure 5. Hodograph derived from the Haskell, Oklahoma wind profiler valid at 2100 UTC 4 May 2003. Data are plotted every 500 m AGL, and filled circles are at every 1 km AGL (units are m s^{-1}). The observed storm motions are plotted for the left- (V_{obs}) and right-

[1] Storm-relative velocity (SRM) data were used to verify the existence of cyclonic (anticyclonic) rotation within the right-moving (left-moving) supercells discussed in the text.

moving (V_{obs}) supercells in northeastern Oklahoma; the forecast supercell motions are plotted for the left- ($V_{LM\text{-}fcst}$) and right-moving ($V_{RM\text{-}fcst}$) supercells using the method of Bunkers et al. (2000); the 0–6-km mean wind is indicated with a filled square; and the shear from the boundary layer to 6 km is represented with a dashed line.

4. STORM INTERACTION

Fig. 6 is a 6-panel radar progression from the WSR-88D radar at Springfield, MO (KSGF) showing the left mover's interaction with the right mover in extreme northeastern Oklahoma and southwestern Missouri. An F1 tornado was reported with the right mover in Ottawa County, Oklahoma around 2300 UTC (near the time in Fig. 6a; tornado location denoted by 'T'), prior to the merger. The left mover had completely intersected the forward flank of the right mover by 2317 UTC (Fig. 6c), before weakening as it continued to the northeast (Figs. 6d-f). During and immediately following the merger, there were no tornado reports. Additionally, the right mover's hook-echo appendage became ill-defined as it crossed into Missouri, then regained its identity by 2347 UTC (Fig. 6f). There were no more tornado reports until 2340 UTC, when the storm was producing an F2 tornado in eastern Newton County (Fig 6f; tornado location denoted by 'T'), and eventually an F3 tornado in Lawrence County. This suggests that the left mover may have temporarily disrupted the tornadic circulation of the right mover.

Both Springfield and Tulsa radars were able to estimate the height of the storm's echo top. At 2305 UTC, just before the interaction, the right mover's overshooting top extended to 17-20 km MSL. By 2315 UTC, the top had decreased to 15.5-18 km MSL, and at 2330 UTC, the highest echo was located 13-16 km MSL. After the interaction, the echo top began increasing again; by 2341 UTC, it was located 16.5-19 km MSL, indicating a very strong updraft had again developed. These data suggest that the right mover's updraft weakened during its interaction with the left mover.

Radar data and tornado reports suggest that the right mover's updraft weakened during and shortly after its interaction with the left mover. Our data are insufficient to conclusively provide a reason for the disruption of the right mover, but here are a few possibilities:

a) Stabilized Inflow

From 2302-2317 UTC, the left mover was producing precipitation in northern McDonald and southern Newton counties (Fig. 6a-c); this is the precise area from which the right mover's inflow originated as it crossed the state border into Missouri. Oklahoma mesonet data (Fig. 7a, b) show that the temperature and dewpoint dropped by approximately 1-2 °C in the wake of the left mover, which is consistent with the detailed analyses of Charba and Sasaki (1971; their Fig. 6). The inflow air for the right mover would therefore be slightly more stable than the ambient air, which could slightly weaken the right mover's updraft.

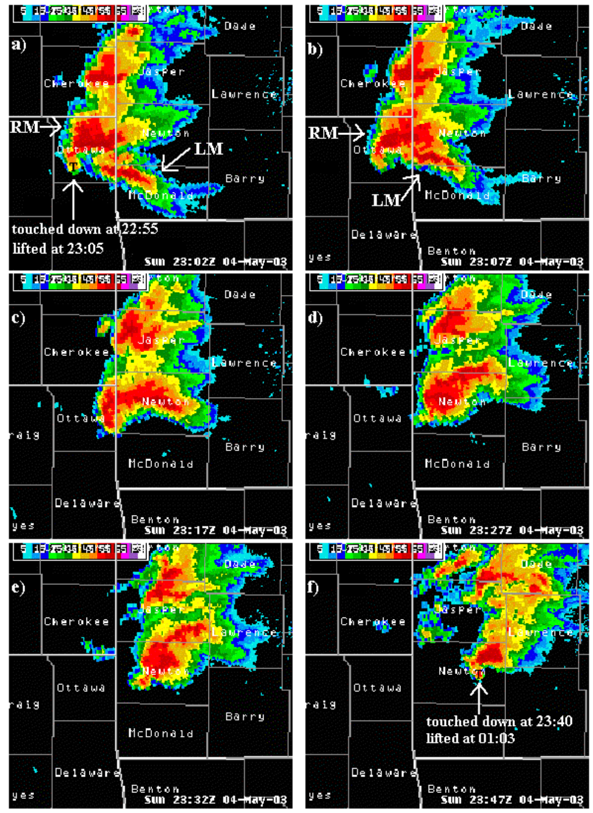

Figure 6. 0.5 degree tilt base reflectivity from the KSGF WSR-88D radar valid at a) 2302 UTC, b) 2307 UTC, c) 2317 UTC, d) 2327 UTC, e) 2332 UTC, and f) 2347 UTC**.** Right mover (left mover) designated by RM (LM). Location of observed tornado indicated with 'T' in a) and f).

b) Vorticity Balance

Radar SRM data from KINX (not shown) confirm that the left mover had an associated meso-anticyclone, i.e., negative vertical vorticity, on the west side of its northern flank. This portion of the storm intersected the right mover on the east side of its mesocyclone, an area of positive vertical vorticity. It stands to reason that these circulations would "cancel each other out," or at least weaken the right mover's circulation. Radial velocity data were poor from both KINX and KSGF, so this hypothesis cannot be confirmed, but it's a logical explanation for the tornadic behavior of the right mover.

c) Natural Pulse in Intensity

The possibility that the right mover was undergoing a natural pulse in intensity as the left mover passed by cannot be ignored. Foote and Frank (1983) found that supercell updrafts occasionally experience fluctuations with no obvious external influence.

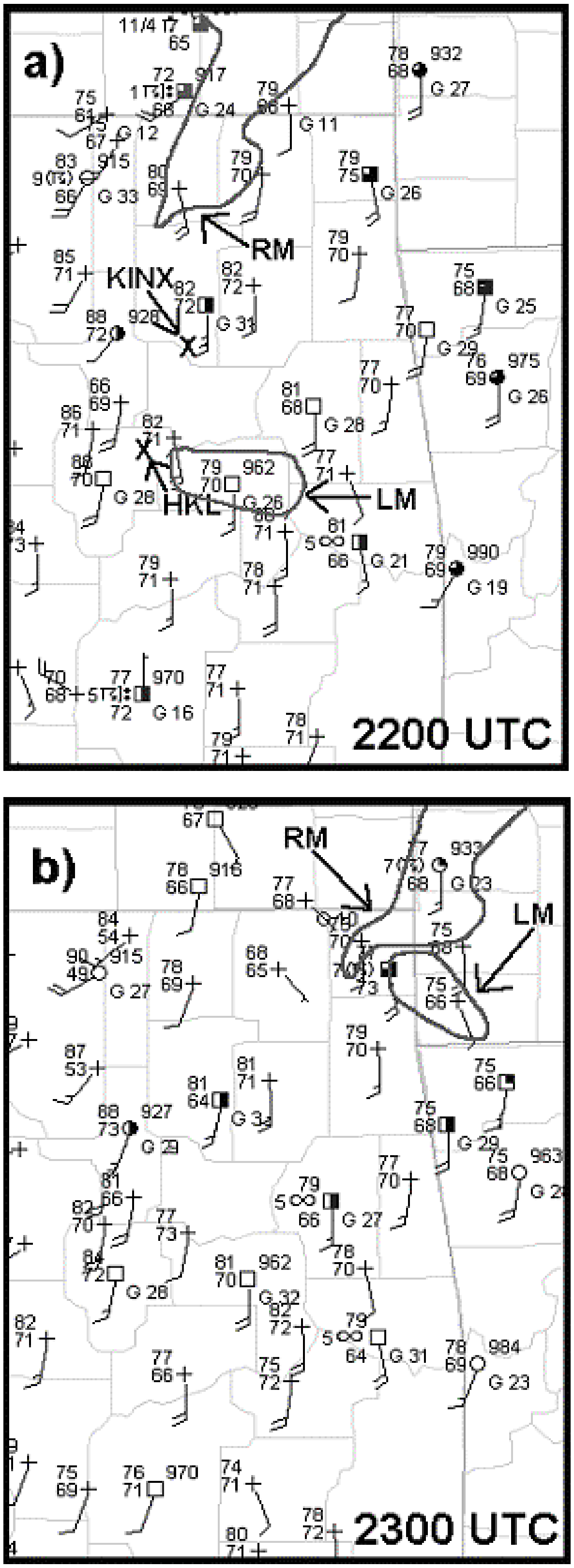

Figure 7. Surface station plots from the Oklahoma mesonet at a) 2200 UTC and b) 2300 UTC. Northeast Oklahoma, northwest Arkansas, southeast Kansas, and southwest Missouri are shown. KINX and HKL show the locations of the Tulsa radar and the Haskell wind profiler, respectively. Dark gray contours show the approximate location of the 25 dBZ 0.5 degree tilt radar contour from KINX for the right mover (RM) and left mover (LM) in northeast Oklahoma which interact shortly after 2300 UTC.

There was at least one other left-moving supercell on this day [moving from 217° at 27 m s^{-1} (53 kt)], and it also intersected, and merged with, an adjacent right-moving supercell in southeastern Kansas. In order to put the present case into better perspective, the occurrence of tornadoes centered around this interaction was also investigated. An F1 tornado was initially reported with the right-moving supercell at 2206 UTC, just prior to the merger with the left mover. The tornado persisted until 2225 UTC, at which time both storms had completely merged near the Missouri border. The right mover subsequently become disorganized and ceased producing tornadoes. The storm then reorganized about 30 minutes after the merger, and produced an F2 tornado from 2304 UTC to 2353 UTC in west-central Missouri. Therefore, this case is similar to the one discussed above in that the supercell was tornadic just prior to merger, became disorganized during and immediately following the merger, but then re-intensified to produce additional strong tornadoes. It is unknown if the two left movers played any role in the re-intensification of these tornadic right movers, or if they just temporarily interrupted an otherwise persistent storm. It is worth noting that both tornadic storms produced long-track tornadoes after the merger.

5. SUMMARY

A left-moving supercell in northeastern Oklahoma on 4 May 2003 was analyzed with respect to its motion, and interaction with another tornadic right-moving supercell. It moved 13 m s^{-1} (26 kt) faster than its right-moving counterpart, and produced very large hail, but no tornadoes. Furthermore, as the left mover interacted with a tornadic right-moving supercell, it seemingly disrupted its rotation, suggesting the merger had a disorganizing effect on the right-mover.

Since this study presents a single example, and little additional information is present in the published literature, mergers between right- and left-moving supercells and the resulting effects on tornadogenesis are topics which deserve further study.

6. REFERENCES

Bluestein, H. B., and S. S. Parker, 1993: Modes of isolated, severe convective storm formation along the dryline. *Mon. Wea. Rev.*, **121**, 1354-1372.

Charba, J., and Y. Sasaki, 1971: Structure and movement of the severe thunderstorms of 3 April 1964 as revealed from radar and surface mesonetwork data analysis. *J. Meteor. Soc. Japan*, **49**, 191-213.

Davies-Jones, R. P., R. J. Trapp, and H. B. Bluestein, 2001: Tornadoes and tornadic storms. *Severe Convective Storms, Meteor. Monogr.,* No. 50, Amer. Meteor. Soc., 167–221.

Dowell, D. C., and H. B. Bluestein, 2002: The 8 June 1995 McLean, Texas, storm. Part I: Observations of cyclic tornadogenesis. *Mon. Wea. Rev.*, **130**, 2626-2648.

Finley, C. A., W. R. Cotton, and R. A. Pielke Sr., 2001: Numerical simulation of tornadogenesis in a high-precipitation supercell. Part I: Storm evolution and transition into a bow echo. *J. Atmos. Sci.*, **58**, 1597-1629.

Foote, G. B., and H. W. Frank, 1983: Case Study of a Hailstorm in Colorado. Part III: Airflow From Triple-Doppler Measurements. *J. Atmos. Sci.*, **40**, 686-707.

Rasmussen, E. N., and D. O. Blanchard, 1998: A baseline climatology of sounding-derived supercell and tornado forecast parameters. *Wea. Forecasting*, **13**, 1148-1164.

Stout, G. E., and H. W. Hiser, 1955: Radarscope interpretations of wind, hail, and heavy rainstorms between May 27 and June 8, 1964. *Bull. Amer. Meteor. Soc.,* **36,** 519-527.

Thompson, R. L., R. Edwards, J. A. Hart, K. L. Elmore, and P. Markowski, 2003: Close proximity soundings within supercell environments obtained from the Rapid Update Cycle. *Wea. Forecasting,* **18,** 1243-1261.